

# NJC

Accepted Manuscript



This is an *Accepted Manuscript*, which has been through the Royal Society of Chemistry peer review process and has been accepted for publication.

*Accepted Manuscripts* are published online shortly after acceptance, before technical editing, formatting and proof reading. Using this free service, authors can make their results available to the community, in citable form, before we publish the edited article. We will replace this *Accepted Manuscript* with the edited and formatted *Advance Article* as soon as it is available.

You can find more information about *Accepted Manuscripts* in the [Information for Authors](#).

Please note that technical editing may introduce minor changes to the text and/or graphics, which may alter content. The journal's standard [Terms & Conditions](#) and the [Ethical guidelines](#) still apply. In no event shall the Royal Society of Chemistry be held responsible for any errors or omissions in this *Accepted Manuscript* or any consequences arising from the use of any information it contains.

## Complexation of Some Alkali and Alkaline Earth Metal Cations by Macrocyclic Compounds Containing Four Pyridine Subunits – a DFT Study

Ines Despotović

*Quantum Organic Chemistry Group, Department of Organic Chemistry and Biochemistry,  
Ruđer Bošković Institute, Bijenička cesta 54, Zagreb 10000, Croatia,*

*E-mail: Ines.Despotovic@irb.hr*

### Abstract:

The thermodynamic properties of the complexes of some alkali and doubly-charged alkaline earth metal cations with tetradentate pyridine-based macrocyclic compounds in the gas phase and in the acetonitrile solution have been established by quantum chemical calculations. It is shown by the reliable DFT B3LYP/6-311+G(3df,2p)//B3LYP/6-31G(d) method that these supramolecular structures act as efficient and very selective scavengers of  $\text{Li}^+$ ,  $\text{Na}^+$ ,  $\text{K}^+$ ,  $\text{Be}^{2+}$ ,  $\text{Mg}^{2+}$  and  $\text{Ca}^{2+}$  metal cations, exhibiting gas phase cation affinities in the range between 58.5 and 553.8 kcal mol<sup>-1</sup> in the sequence  $\text{K}^+ < \text{Na}^+ < \text{Li}^+ < \text{Ca}^{2+} < \text{Mg}^{2+} < \text{Be}^{2+}$ . The structures of the uncomplexed and complexed ligands are provided and the changes of the macrocyclic ring conformation and the geometrical response of the ligand binding site to the varying guests has been analyzed. The charge transfer process and nature of the interactions in the formed complexes has been investigated. The results revealed that metal cations act as charge acceptors and the amount of charge transfer is in agreement with the cation affinities. The bond order analysis shows medium strength covalent interactions between the four pyridine nitrogen atoms and the metal cation in complexes with  $\text{Be}^{2+}$ , while the smallest covalent interaction was found for  $\text{K}^+$  complexes. The cation affinity of the ligands is amplified by attaching electron-donating substituents to the pyridine rings. The solvent effects were assessed using the polarized continuum method (PCM). The complexation order was preserved in acetonitrile solution.

Keyword: macrocyclic ligand, pyridine, metal cation, complexation, DFT, solvent effect

## 1. Introduction

Since the early work of Pederson, who reported a cyclic polyether capable of forming stable complexes with many salts of alkali and alkaline earth metals,<sup>1</sup> the interest in supramolecular chemistry or host-guest chemistry has been rapidly increased. The ability of macrocyclic ligands to bind metal ions selectively<sup>2</sup> has proved very useful in ion transport,<sup>3</sup> chemosensing,<sup>4</sup> metalloenzyme mimics,<sup>5</sup> catalysis,<sup>6</sup> and nuclear waste treatment.<sup>7</sup> Furthermore, macrocyclic ligands as metal-protein attenuating compounds have recently been proposed as potentially therapeutic in Alzheimer disease.<sup>8</sup>

Among a large variety of macrocycles synthesized as scavengers of metal ions those containing pyridine building fragments have attracted considerable attention.<sup>9</sup> Introduction of the pyridine moiety strongly influences the thermodynamic properties and complexation kinetics by increasing the conformational rigidity and changing its basicity. Pyridine-containing macrocycles are readily accessible and versatile platforms that give rise to a variety of structural motifs, three-dimensional cages, sterically enforced macrocycles, and ligands with additional functional groups attached to the macrocycles.<sup>10</sup> The smaller homologues are generally highly rigid and, with a conformationally preorganized active site, they may give complexes of high thermodynamic stability. In terms of a size-matching effect, they are especially suitable for small metal cations. Recently, we have examined the interaction of the small Be<sup>2+</sup> metal cation with some derivatives of small, rigid and well preorganized *N*-(phenyl) substituted azacalix[3](2,6)pyridine, prepared by Kanbara et al.,<sup>11</sup> and have reported a very high cationic affinity CA(Be<sup>2+</sup>) of 544.9 kcal mol<sup>-1</sup> for the hexadimethylamino derivative.<sup>12</sup>

In the present work, we study the complexation of previously described conformationally rigid, pyridine-based, four-fragment macrocycles<sup>13</sup> (Figure 2) with the first few monocharged alkali and doubly-charged alkaline earth metal cations. By using the DFT approach, we show that these macrocyclic systems are very promising as candidates for selective and efficient metal cation scavengers of Li<sup>+</sup>, Na<sup>+</sup>, K<sup>+</sup>, Be<sup>2+</sup>, Mg<sup>2+</sup> and Ca<sup>2+</sup>. The study revealed gas phase cation affinities in the range between 58.5 and 553.8 kcal mol<sup>-1</sup>. The geometrical and electronic structure of uncomplexed and complexed ligands were investigated, and charge transfer values together with strength of covalent bonds were determined. The binding ability of pyridine-based macrocycles was examined in acetonitrile solution using the PCM method.

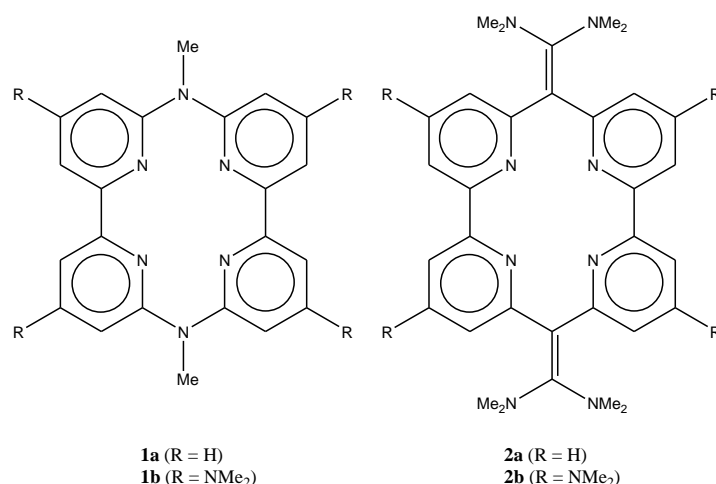


**Figure 1** Structural formula of macrocyclic systems **1** and **2**.

The calculated  $\log K$  values are found to range from 8.36 to 52.05 units. Both, in the gas phase and in the solution the most strongly complexed cation was found to be  $\text{Be}^{2+}$ .

## 2. Theoretical framework and computational procedure

The gas phase complexation enthalpies,  $\Delta_r H_{\text{complex}}$ , are calculated according to Eq. 1:

$$\Delta_r H_{\text{complex}} = \Delta_f H(\text{SM})^{+/2+} - [\Delta_f H(\text{S}) + \Delta_f H(\text{M}^{+/2+})] \quad (1)$$

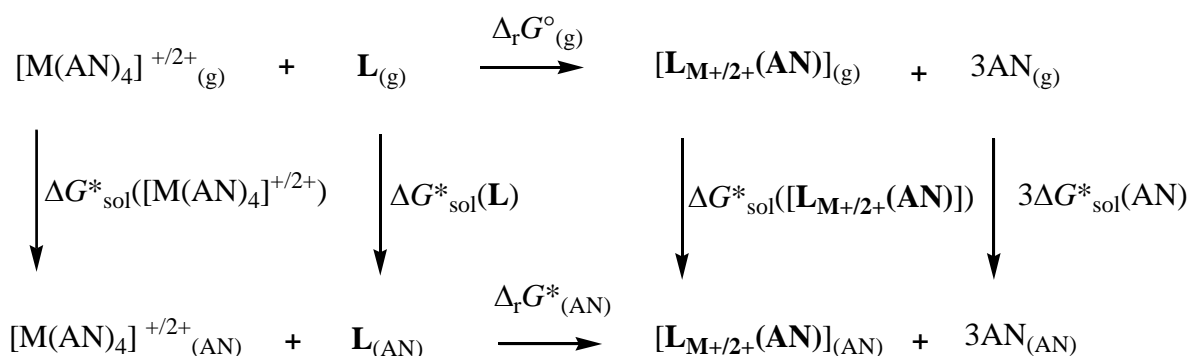
where S stands for a supramolecule,  $\text{M}^{+/2+}$  represents the metal ion, and  $\Delta_f H$  is the enthalpy of formation. It involves the electronic energy, the zero point vibrational energy a thermal correction to room temperature. An equivalent equation is used for the Gibbs free energies  $\Delta_r G_{\text{complex}}$ . The B3LYP<sup>14</sup> density functional has been selected as the method of choice. The geometry optimizations were performed with the efficient 6-31G(d) basis set. The B3LYP/6-31G(d) level of theory is known to give accurate results for the geometries of a wide variety of systems, including in particular, complexes of metal cations with organic bases.<sup>15</sup> ZPVEs and thermal corrections were extracted from the corresponding frequency calculations without the application of scaling factors. The final molecular energies were obtained by the large and highly flexible 6-311+G(3df,2p) basis set. This give rise to the reliable B3LYP/6-311+G(3df,2p)//B3LYP/6-31G(d) model<sup>16</sup> employed here. No pseudo-potentials have been used for the metal cations. The binding energies were corrected for the basis set superposition

error (BSSE) calculated by the counterpoise (CP)<sup>17</sup> scheme at the B3LYP/6-311+G(3df,2p)//B3LYP/6-31G(d) level of theory. The BSSE errors were found to be very small so they may be safely omitted in further calculations of binding energies for similar systems with methods of the same quality. The cation affinities (CA) and cation basicities (CB) are defined as negative values of  $\Delta_r H_{\text{complex}}$  and  $\Delta_r G_{\text{complex}}$ , respectively, as calculated from Eq. 1. Basicity values are given in order to make more facile comparison with future experiments.

The strength of the metal cation binding in the condensed phase is the result of the competitive processes of desolvation of the reagents, binding of the metal cation, solvation of the product and reorganization of the solution. Solvation effects were taken into account in a double way: (a) considering the dissociation of the solvent molecules (AN) from the first coordination sphere of the metal ion, (b) employing the polarizable continuum model (PCM) introduced by Miertuš, Scrocco and Tomasi.<sup>18</sup> Calculations in PCM acetonitrile solvent were carried out using gas phase minimum structures without further optimization during the evaluation of the free energy of solvation using B3LYP/6-311+G(d,p). The gas phase vibrational contributions were added to the appropriate single-point energies from the solution phase. Recently it was shown that when the liquid and gas phase solute structures are similar, it is a correct and useful approach to use gas-phase geometries and frequencies in computing free energies of solutes in solution.<sup>19</sup> The true minima on the potential energy surface at the B3LYP/6-311+G(d,p) level of theory were verified for solutes. The acetonitrile (AN) solvent is represented by a polarizable continuum characterized by a dielectric constant of 36.64. The solute cavity is constructed by overlapping atom-centered spheres of 1.0 Å radii. To account for the specific interaction of metal cation with AN solvent, the first solvation shell,<sup>20</sup> represented by four AN molecules<sup>21</sup> (in tetrahedral coordination with a nitrogen atom pointing to  $M^{+/2+}$  cation) is explicitly included in the quantum chemical region and the remaining bulk solvent is approximated by a polarizable continuum, leading to the cluster continuum method.<sup>22</sup> Also, specific coordination of acetonitrile to the complexes of macrocyclic systems **1** and **2** have been taken into account by explicitly including one AN molecule giving rise to penta coordinated metal cations. This kind of coordination has been reported by several authors.<sup>23</sup> The stability constant was calculated utilizing the well-known relation,  $\Delta_r G^* = -RT \ln K$ . The thermodynamics is based on the following process:



where " $M^{+/2+}$ " stands for the metal cation, " $L$ " stands for the macrocyclic ligand, whereas " $AN$ " indicates solvation in acetonitrile. Using the thermodynamic cycle given in Scheme 1



**Scheme 1.** Thermodynamic cycle used in calculation of  $\Delta_r G^*_{(AN)}$  of complexation of  $L$  ( $L = 1a, 2a, 1b$  and  $2b$ ) with  $M^{+/2+}$ .

$\Delta_r G^*_{(AN)}$  is calculated *via* the gas phase complexation free energy,  $\Delta_r G^{\circ}_{(g)}$ , which, in turn, is calculated as stated in Equation 3:

$$\Delta_r G^{\circ}_{(g)} = \Delta_f G^{\circ}([L_{M+/2+}(AN)]) + 3 \Delta_f G^{\circ}(AN) - [\Delta_f G^{\circ}([M(AN)_4]^{+/2+}) + \Delta_f G^{\circ}(L)] \quad (3)$$

where  $\Delta_f G^{\circ}$  is the free energy of the formation. It involves the electronic energy, the zero-point vibrational energy contribution and thermal corrections to 298.15 K. All species were immersed in the AN solvent and their solvation free energies were added to the gas phase reaction free energy to obtain  $\Delta_r G^*_{(AN)}$ :

$$\Delta_r G^*_{(AN)} = \Delta_r G^{\circ}_{(g)} + \Delta G^{\circ}_{sol}(L_{M+/2+}) + 3\Delta G^{\circ}_{sol}(AN) - \Delta G^{\circ}_{sol}([M(AN)_4]^{+/2+}) - \Delta G^{\circ}_{sol}(L) + 2\Delta G^{\circ \rightarrow *} \quad (4)$$

where  $\Delta G^{\circ}_{sol}(L_{M+/2+})$  is the solvation free energy of the complex in AN solvent,  $\Delta G^{\circ}_{sol}(AN)$  represents the solvation of AN molecules in AN solvent,  $\Delta G^{\circ}_{sol}([M(AN)_4]^{+/2+})$  is solvation free energy of clustered metal cation in AN solvent,  $\Delta G^{\circ}_{sol}(L)$  is solvation free energy of macrocyclic ligand in AN solvent, and  $\Delta G^{\circ \rightarrow *}$  represents the free energy change of 1mol of an ideal gas from a 1 atm to a 1M standard state. It was applied to each gas phase reactant and product. At 298K,  $\Delta G^{\circ \rightarrow *}$  has value of 1.89 kcal mol<sup>-1</sup>.<sup>24</sup> All calculations were performed using the GAUSSIAN 03 program package.<sup>25</sup>

### 3. Results and Discussion

#### 3.1. Gas phase complexation

##### 3.1.1. Cation affinity and basicity

Important information of the ion-base interaction can be obtained by investigation of the thermodynamics of this process in the gas phase, which is free from the influence of solvent and counter ions. The macrocyclic systems studied here are given in Figure 1, while the  $\text{Li}^+$ ,  $\text{Na}^+$ ,  $\text{K}^+$ ,  $\text{Be}^{2+}$ ,  $\text{Mg}^{2+}$  and  $\text{Ca}^{2+}$  cation affinities and basicities of pyridine, *para* NMe<sub>2</sub> substituted pyridine (4-dimethylaminopyridine, 4-DMAP), hereafter denoted by DMAP, as well as of **1a** - **2b** ligands, are listed in Table 1. The electronic energies, thermal corrections to the enthalpies and Gibbs free energies, as well as basis set superposition errors, are given in Table S2. The cation affinity and basicity are calculated by using Eq. 1 for affinity and its analog for basicity.

The building-block pyridine compound has relatively low cation affinities CA, of 46.0, 32.0, 22.0, 221.0, 129.9 and 88.5 kcal mol<sup>-1</sup>, for  $\text{Li}^+$ ,  $\text{Na}^+$ ,  $\text{K}^+$ ,  $\text{Be}^{2+}$ ,  $\text{Mg}^{2+}$  and  $\text{Ca}^{2+}$ , respectively, as calculated by the B3LYP/6-311+G(3df,2p)//B3LYP/6-31G(d) method. DMAP has higher cation affinities for  $\text{Li}^+$ ,  $\text{Na}^+$ ,  $\text{K}^+$ ,  $\text{Be}^{2+}$ ,  $\text{Mg}^{2+}$  and  $\text{Ca}^{2+}$  by 16.8, 8.8, 7.5, 42.8, 30.7 and 25.9 kcal mol<sup>-1</sup>, respectively (Table 1), compared to pyridine. The reason for this is considered to be due to the electron releasing property of the nitrogen lone pair of the NMe<sub>2</sub> group and its contribution to the cationic resonance triggered by metal cation complexation and spread over the pyridine ring from the complexation site.

Significant changes have been observed when four pyridine rings coordinate the metal cation in a tetrahedral fashion. The binding affinities are 115.7, 87.4, 62.9, 482.3, 331.2 and 241.9 kcal mol<sup>-1</sup> for  $\text{Li}^+$ ,  $\text{Na}^+$ ,  $\text{K}^+$ ,  $\text{Be}^{2+}$ ,  $\text{Mg}^{2+}$  and  $\text{Ca}^{2+}$ , respectively, being enlarged to values of 134.3, 104.7, 79.0, 539.3, 384.2 and 291.0 kcal mol<sup>-1</sup> when pyridine molecules are replaced by DMAP. These affinities are roughly two or three times larger than those of the metal cations coordinated by a single pyridine molecule.

The tetrapodal interactions between macrocyclic systems **1a** - **2b** and the cations are similar to those in  $[\text{M}(\text{Py})_4]^{+/2+}$ , with the CA ranging from 58.5 to 553.8 kcal mol<sup>-1</sup>. The destabilization effects in the complexes, due to distortion from the ideal coordination geometry, are prevailed by the following stabilization effects operating here: (a) the chelate

effect<sup>26</sup> which accounts for an increase in CA of chelating ligands for a metal ion compared to the affinity of a collection of similar nonchelating (monodentate) ligands, (b)

**Table 1** The cation  $\text{Li}^+$ ,  $\text{Na}^+$ ,  $\text{K}^+$ ,  $\text{Be}^{2+}$ ,  $\text{Mg}^{2+}$  and  $\text{Ca}^{2+}$  affinities and basicities of pyridine, and **1a** - **2b** ligands calculated using the B3LYP/6-311+G(3df,2p)//B3LYP/6-31G(d) method (in  $\text{kcal mol}^{-1}$ ).

Compd	Cations	$\text{Li}^+$	$\text{Na}^+$	$\text{K}^+$	$\text{Be}^{2+}$	$\text{Mg}^{2+}$	$\text{Ca}^{2+}$
Py	CA	46.0	32.0	22.0	221.0	129.9	88.5
	CB	38.7	25.1	15.6	213.2	122.3	81.4
DMAP	CA	56.8	40.8	29.5	263.8	160.6	114.4
	CB	49.4	33.8	23.0	256.2	153.8	107.6
<b>1a</b>	CA	123.1	82.9	58.5	484.6	331.5	237.4
	CB	113.3	72.8	48.9	473.1	320.2	226.9
<b>1b</b>	CA	142.6	100.9	74.8	540.0	382.3	284.2
	CB	133.5	91.6	66.2	529.5	371.9	274.1
<b>2a</b>	CA	133.1	90.1	64.5	521.6	371.6	264.5
	CB	123.0	80.2	55.7	510.8	360.9	253.7
<b>2b</b>	CA	144.0	100.9	75.2	553.8	401.1	292.7
	CB	133.5	91.4	67.0	544.2	390.5	282.6

CA and CB denote cation affinity and basicity, respectively.

macrocyclic effect,<sup>27</sup> which accounts for the increase in CA due to the fact that the polydentate ligand is constructed like a ring compound, with several donor atoms that can bind the Lewis acid inside the ring, as well as (c) the high level of preorganization,<sup>28</sup> which means that free ligand is very close in its structure to that required for complexation of the target metal ion, thus facilitating the said complexation.



The size-match selectivity, the idea that a metal ion will form its most stable complex with a macrocycle where the sizes of the metal ion and the macrocyclic cavity are most closely matched, is generally accepted<sup>29</sup> to be the most important factor in controlling metal ion selectivity in macrocyclic ligands. It plays its greatest role when the ligands are relatively inflexible.<sup>30</sup> Closely related to the metal-ion size is the chelate-ring size effect that states<sup>31</sup> that the increase of the chelating ring size, from five- to six-membered, in a complex will increase the stability of complexes of smaller relative to larger metal ions. In the presented systems, with two five- and two six-membered chelate rings, the small metal cations coordinate best in six-membered chelate rings, while the two five-membered chelate rings destabilize the macrocycle. On the other hand, the larger metal cations coordinate best in five-membered chelate rings, while the two six-membered chelate rings will destabilize the system. Consequently, the overall effect of the chelate ring size on the stability of the complex is expected to be practically the same in complexes with small and large metal cations.

The CA values of macrocyclic system **1a** (Figure 1) comprising four pyridine moieties connected by two C(sp<sup>2</sup>)-C(sp<sup>2</sup>) biphenyl-type bonds and two NMe bridges, towards Li<sup>+</sup>, Na<sup>+</sup>, K<sup>+</sup>, Be<sup>2+</sup>, Mg<sup>2+</sup> and Ca<sup>2+</sup> cations are 123.1, 82.9, 58.5, 484.6, 331.5 and 237.4 kcal mol<sup>-1</sup>, respectively. A quadruple substitution at the para positions of the pyridine rings by electron donating NMe<sub>2</sub> groups in **1b** additionally increases the CA by 19.5, 18.0, 16.3, 55.4, 50.8 and 46.8 kcal mol<sup>-1</sup> in **1b**<sub>Li+</sub>, **1b**<sub>Na+</sub>, **1b**<sub>K+</sub>, **1b**<sub>Be2+</sub>, **1b**<sub>Mg2+</sub> and **1b**<sub>Ca2+</sub> (Table 1), respectively. This is due to the contribution of the nitrogen lone pair of the NMe<sub>2</sub> groups to the cationic resonance upon complexation. The highest cation affinity, of 540.0 kcal mol<sup>-1</sup>, is calculated for the Be<sup>2+</sup> cation. This spectacular CA(Be<sup>2+</sup>) affinity is expected, because Be<sup>2+</sup> is a dication, having a very high electron affinity<sup>32</sup> of 635.0 kcal mol<sup>-1</sup> and the smallest radius<sup>33</sup> of only 0.59 Å, enabling a perfect fitting within the investigated macrocyclic ion-binding site formed by four inward oriented pyridine nitrogen atoms, as depicted in Figure 1. The corresponding cation affinity CA(Mg<sup>2+</sup>) is dramatically smaller, being 382.3 kcal mol<sup>-1</sup> for the tetradentate ligand **1b**. It follows that the Mg<sup>2+</sup> affinity is decreased by 157.7 kcal mol<sup>-1</sup>, which is not surprising in light of the fact that Mg<sup>2+</sup> has an electron affinity that is 112.0 kcal mol<sup>-1</sup> lower than that of Be<sup>2+</sup>, being 523.0 kcal mol<sup>-1</sup>,<sup>32</sup> and a larger radius (0.86 Å).<sup>33</sup> The Ca<sup>2+</sup> cation has an electron affinity of 414.8 kcal mol<sup>-1</sup><sup>32</sup> and a radius of 1.14 Å,<sup>33</sup> which results in CA(Ca<sup>2+</sup>) for the ligand **1b** of 284.2 kcal mol<sup>-1</sup>. The same argument holds for the Li<sup>+</sup>, Na<sup>+</sup> and K<sup>+</sup> cations, albeit to a much greater extent. To be more specific, the electron affinity of the Na<sup>+</sup>, Li<sup>+</sup> and K<sup>+</sup>

cations<sup>32</sup> are much lower than that of the  $\text{Be}^{2+}$ , being 124.3, 118.4 and 100.1 kcal mol<sup>-1</sup>, and larger radii, of 0.90, 1.16 and 1.52 Å, respectively.<sup>33</sup> As a consequence, the cation affinities of  $\text{Li}^+$ ,  $\text{Na}^+$  and  $\text{K}^+$  of the ligand **1b** are lower than that of  $\text{Be}^{2+}$  by 397.4, 439.1 and 465.2 kcal mol<sup>-1</sup>, respectively, as calculated by the B3LYP/6-311+G(3df,2p)//B3LYP/6-31G(d) method (Table 1). Based on these results, it is clear that electron affinity and cationic radius correlate very well with cation affinity of the ligands **1a** – **1b**. The CA increases with the decrease of the radius and the increase of the electron affinity of the metal cation. As shown, the highest values of the cation affinities are found to be for the  $\text{Be}^{2+}$  cation, while the lowest values are found for  $\text{K}^+$ . The  $\text{Be}^{2+}$  cation, with its smallest radius is the most suitable among the considered cations for macrocycle **1** and, as depicted in Figure S43, it forms the most stable complexes. On the contrary,  $\text{K}^+$  is a clear misfit for the cavity, thus forming the least stable complexes. These findings clearly confirm that, for alkali and alkaline earth metal cations, the increase in the atomic number within the same group of elements is accompanied by a decrease in the binding energy.<sup>34</sup> It has to be noted that the CA values are much larger in the alkaline earth metal cation complexes than in alkali metal cation complexes. These large differences in CA values can be attributed to the increased charge and charge density (charge-to-size ratio) being present on the alkaline earth metal cations, as compared with the alkali metal cations.<sup>35</sup> This is one of the very important factors influencing the strength of binding.<sup>36</sup> The differences occur because the smaller metal ions of the same formal charge create a stronger electrostatic field, due to a greater charge density, which results in the formation of more stable complexes. As shown, the same trend in CA values, with respect to change in charge density of the metal cation, was observed for  $\text{Li}^+$  to  $\text{K}^+$  as for  $\text{Be}^{2+}$  to  $\text{Ca}^{2+}$ .

The system of compounds formed by framework **2** provides, in general, stronger ligands (Table 1) compared to those of framework **1**. It appears that unsubstituted macrocycle **2a** has larger CAs for  $\text{Li}^+$ ,  $\text{Na}^+$  and  $\text{K}^+$  cations by only 10.0, 7.2 and 6.0 kcal mol<sup>-1</sup>, respectively, than its counterpart **1a**. However, the CAs for  $\text{Be}^{2+}$ ,  $\text{Mg}^{2+}$  and  $\text{Ca}^{2+}$  of **2a** are of considerably higher values than those of **1a** by 37.0, 40.1 and 27.1 kcal mol<sup>-1</sup>, respectively. Further, the CAs of the substituted derivative **2b** for  $\text{Li}^+$ ,  $\text{Na}^+$  and  $\text{K}^+$  are additionally enlarged by 10.9, 10.8 and 10.7 kcal mol<sup>-1</sup>, respectively, compared to those of **2a**. They approach slightly higher or exactly the same values as those of **1b**, while the CAs for  $\text{Be}^{2+}$ ,  $\text{Mg}^{2+}$  and  $\text{Ca}^{2+}$  are higher by 32.2, 29.5 and 28.2 kcal mol<sup>-1</sup>, respectively, compared to those of **2a**, exceeding the values **1b**<sub>Be2+</sub>, **1b**<sub>Mg2+</sub> and **1b**<sub>Ca2+</sub> by 13.8, 18.8 and 8.5 kcal mol<sup>-1</sup>, respectively.

A very respectable CA value of 553.8 kcal mol<sup>-1</sup> of ligand **2b** towards Be<sup>2+</sup> has to be highlighted.

### 3.1.2. Structural features

We will now turn to the salient structural features of compounds **1a** - **2b** and their complexes, starting with the metal complex of pyridine and their *para*-dimethylamino derivatives. The structures of uncomplexed and complexed ligands are depicted, along with their cartesian coordinates, in Figures S1-S42.

Let us begin by considering the complexes of building block pyridine with the chosen metal cations. Bonding at nitrogen produces reorganization of the electron density over the ring  $\pi$ -network from the pyridine nitrogen in a typical alternating way by stretching and shrinking neighboring bonds, as indicated by the cationic resonance structure (Figure 2). The largest changes in the bond distances are found in N-C bonds, while the less intensive changes in the bond distances are found in bonds more distant from the pyridine nitrogen. The reorganization of the electron density is the most intensive in complex with Be<sup>2+</sup>, meaning that the bonds are shortened and stretched to the highest extent, while the less intensive changes are found in the complex with Na<sup>+</sup> ion. Further, the pyridine nitrogen – metal cation distance is the shortest in the complex with Be<sup>2+</sup>, while the corresponding distance is the largest in complex of pyridine with K<sup>+</sup>.

The influence of the *para* substituted NMe<sub>2</sub> group on the pyridine ring is as follows. There is an electron releasing resonance interaction of the NMe<sub>2</sub> nitrogen with the aromatic ring in the *para* NMe<sub>2</sub> substituted pyridine, which affects its bond distances, in spite of the fact that the N-Me bonds are rotated out of the ring plane by  $\pm 7^\circ$ , and that the nitrogen atom is slightly pyramidal (Figure S8). Complexation of the *para* NMe<sub>2</sub> substituted pyridine produces considerable reorganization of the electron density *via* amplified cationic resonance, which significantly shortens the Me<sub>2</sub>N-C distance. Since the NMe<sub>2</sub> nitrogen participates in the resonance interaction by increasing the double bond character of the Me<sub>2</sub>N-C bond, its  $\pi$ -electron is less available for the hyperconjugate interactions with the Me groups, which, in turn, takes place in the neutral molecule. Consequently, the N-Me bond lengths should be increased, which indeed occurs (Figure 2). This is one of the characteristic features of cationic resonance triggered by cation bonding when NMe<sub>2</sub> substituents are present. Thus, it could serve as one of its fingerprints. At the same time, the N-M<sup>+2+</sup> distance becomes shorter than in analogous complexes without the NMe<sub>2</sub> group, the exception being the complex with Mg<sup>2+</sup>.

Let us continue the discussion with the superstructure **1a** and its complexes (Figure 3). The first observation made is that the molecule **1a** is significantly non-planar (Figure S15). The rings I and II are rotated by a dihedral angle of  $-47.2^\circ$ . Rings I and III are equivalent and the same holds for rings II and IV. On the contrary, the rings I and IV (and rings II and III) differ, and their conjugation interaction with N5 is asymmetric. The  $\pi$ -conjugation between C(I) and N5 is weaker than between C(IV)-N5, which results in a longer C(I)-N5 distance, and a larger N1-C(I)-N5-C(IV) torsional angle, compared with the C(IV)-N5 distance and the N4-C(IV)-N5-C(I) dihedral angle. The same holds in symmetrical fashion for the

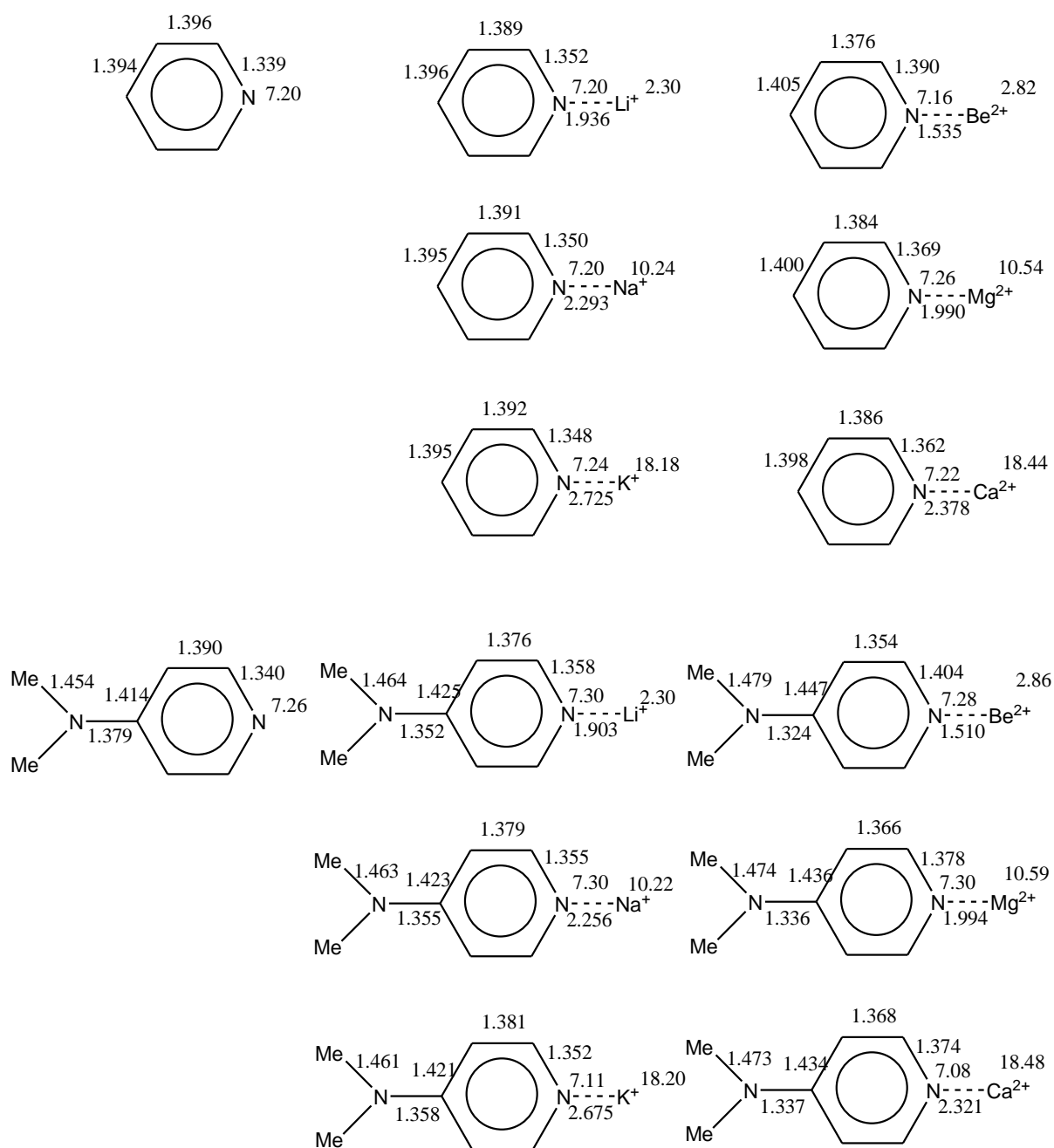


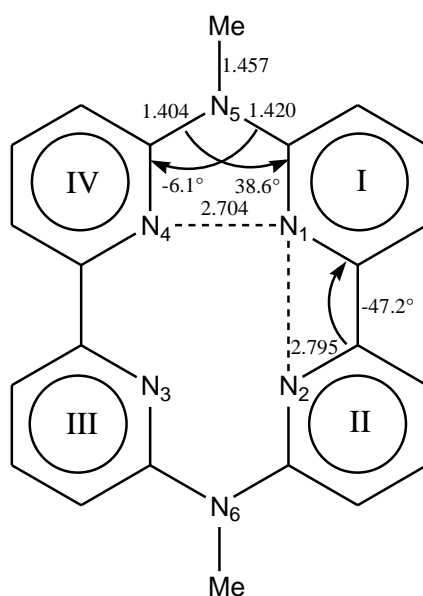
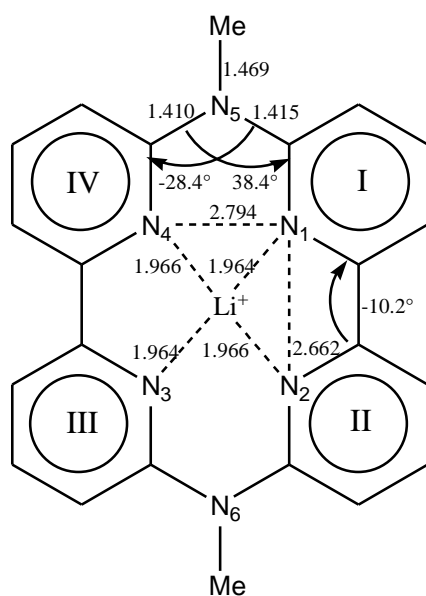
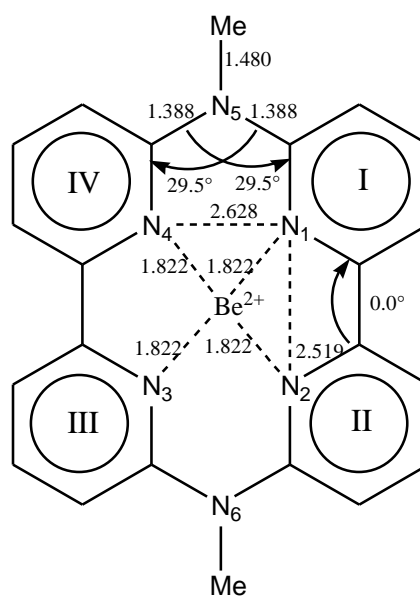
**Figure 2** Some relevant structural parameters (in Å) of pyridine, DMAP and their complexes with  $\text{Li}^+$ ,  $\text{Na}^+$ ,  $\text{K}^+$ ,  $\text{Be}^{2+}$ ,  $\text{Mg}^{2+}$  and  $\text{Ca}^{2+}$ , and Hirshfeld populations (in  $e$ ) of pyridine nitrogens and metal cations.

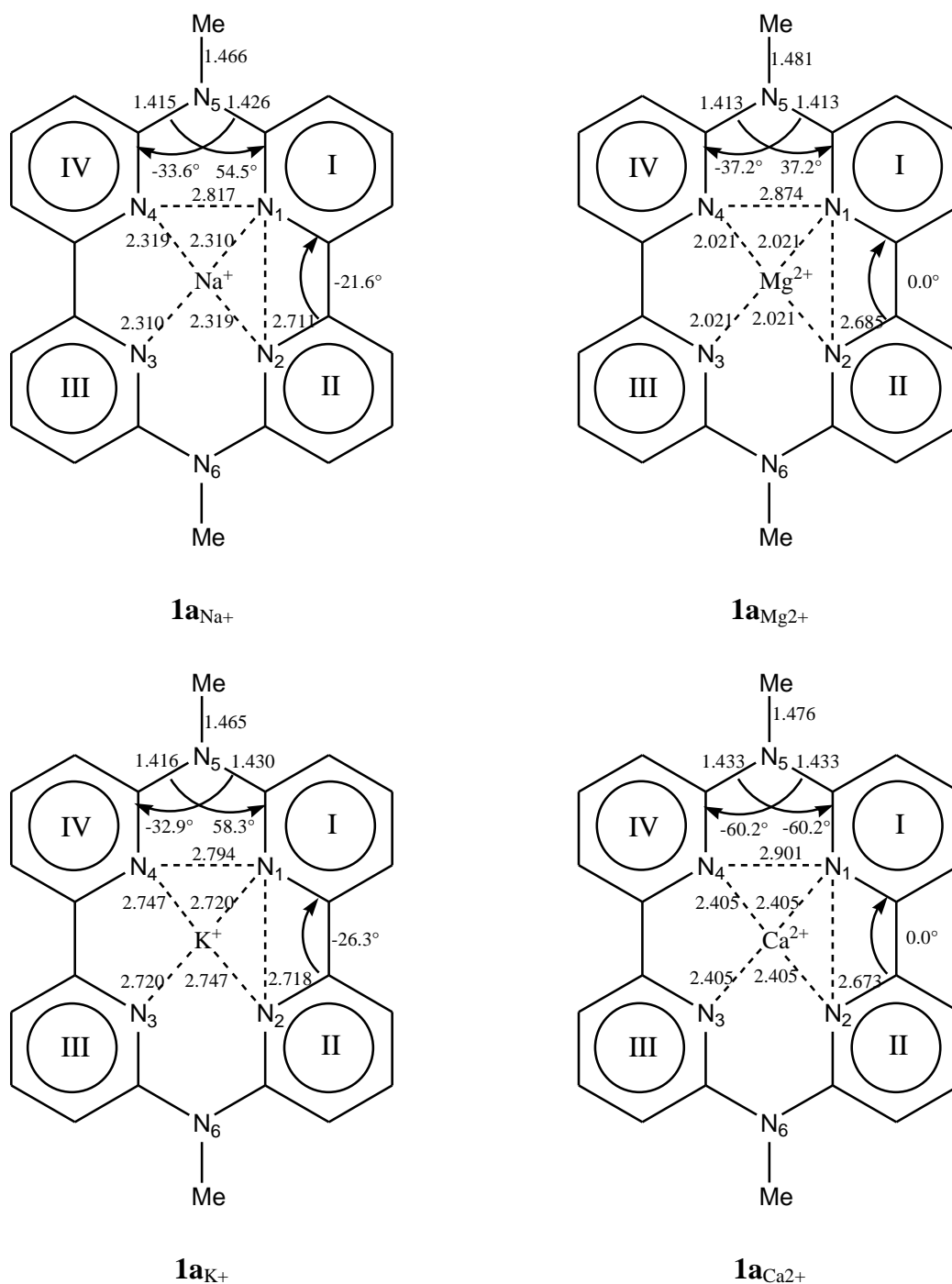
remaining part of the molecule consisting of pyridine rings II and III connected by the NMe bridge. The **1a** cooperatively acts in a tetradentate fashion, providing four pyridine nitrogen atoms to bind to a central atom in a coordination complex. As a highly preorganized ligand, it holds two directly connected pyridine subunits in a conformation with N donor atoms *cis* to each other, which is exactly the conformer required for complex formation. On the other hand, as supported by numerous crystal structures,<sup>37</sup> the two directly connected pyridine rings exclusively adopt the *trans* conformation when part of a free unit.

The dihedral angles between directly connected pyridine rings are substantially decreased (in absolute values) upon complexation in **1a**<sub>Be2+</sub> (Figure 3), assuming values of 0.0°. The cationic resonance between pyridine rings I and IV is evidenced by the decrease in the bond distances C(I)-N5 and C(IV)-N5. The torsion angles N1-C(I)-N5-C(IV) and N4-C(IV)-N5-C(I) are equalized, assuming a value of 29.5°. As a consequence the N····N non-bonded contacts in **1a**<sub>Be2+</sub> are considerably shortened compared with their **1a** analogs. The  $\text{Be}^{2+}$  cation is separated from the four pyridine nitrogen donors by 1.822 Å and fits the macrocyclic binding site quite well (Figure S19). The  $\text{Mg}^{2+}$  cation is positioned at somewhat larger distances from the pyridine nitrogens. At the same time, the non-bonded N····N distances are longer compared with their analogues in **1a**<sub>Be2+</sub>. Again, the rings I and II lie in the same plane, as do rings III and IV. The  $\pi$ -conjugation between the C(I) and N5 atoms, as well as between the C(IV) and N5 atoms, is weaker, which is reflected in longer C(I)-N5 and C(IV)-N5 bond distances and greater torsional angles (N1-C(I)-N5-C(IV) and N4-C(IV)-N5-C(I)). The distances between the  $\text{Ca}^{2+}$  cation and the pyridine nitrogens are larger compared to those between  $\text{Mg}^{2+}$  and the pyridine nitrogens. The N····N distances, as well as the C(I)-N5 and C(IV)-N5 distances are also larger, together with greater torsional angles N1-C(I)-N5-C(IV) and N4-C(IV)-N5-C(I) compared with those in **1a**<sub>Mg2+</sub>.

The structural parameters in **1a**<sub>Li+</sub>, **1a**<sub>Na+</sub> and **1a**<sub>K+</sub> follow the same trend as in **1a**<sub>Be2+</sub>, **1a**<sub>Mg2+</sub> and **1a**<sub>Ca2+</sub>. The only appreciable difference concerns the dihedral angles between directly connected pyridine rings. In the **1a**<sub>Be2+</sub>, **1a**<sub>Mg2+</sub> and **1a**<sub>Ca2+</sub> complexes, their values are 0.0°, while in **1a**<sub>Li+</sub>, **1a**<sub>Na+</sub> and **1a**<sub>K+</sub> a notable internal rotation is observed. The degree of internal rotation is increased as the complexing metal cation becomes larger.

It should be noted in passing that the N5-Me bonds are lengthened to a certain extent upon complexation in **1a**<sub>Be2+</sub>, **1a**<sub>Mg2+</sub>, **1a**<sub>Ca2+</sub>, **1a**<sub>Li+</sub>, **1a**<sub>Na+</sub> and **1a**<sub>K+</sub> (Figure 3). This is a consequence of diminishing hyperconjugative interactions between the methyl groups and the lone pairs of the amino nitrogens, upon complexation.

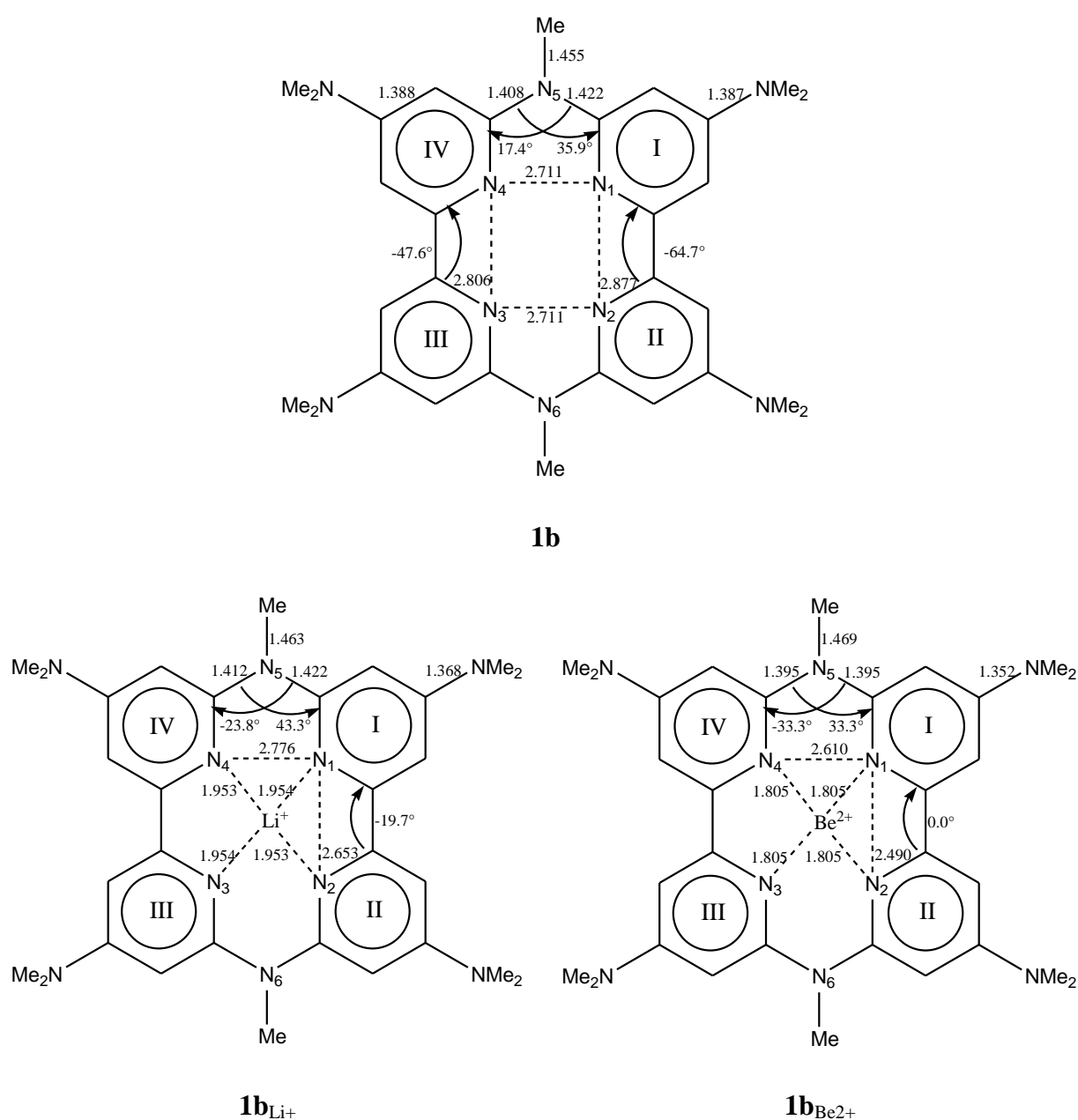
**1a****1a**<sub>Li+</sub>**1a**<sub>Be2+</sub>



**Figure 3** Some relevant structural parameters of supramolecule **1a** and its complexes with  $\text{Li}^+$ ,  $\text{Na}^+$ ,  $\text{K}^+$ ,  $\text{Be}^{2+}$ ,  $\text{Mg}^{2+}$  and  $\text{Ca}^{2+}$  (bond distances are given in Å).

The striking feature of the fourfold *para* NMe<sub>2</sub> substituted superstructure **1b** (Figure 4) is its greater nonplanarity compared to **1a**. The rings I and II are rotated by a dihedral angle relative to each other that is 15.5° higher than in **1a**, resulting in an increase of the non-bonded N····N contacts. The dihedral angle between the two directly connected pyridine rings

is substantially decreased (in absolute value) upon complexation in **1b** complexes (Figure 4). The nitrogen - metal cation distances of the complexes of **1b** with  $\text{Li}^+$ ,  $\text{Na}^+$ ,  $\text{K}^+$ ,  $\text{Be}^{2+}$ ,  $\text{Mg}^{2+}$  and  $\text{Ca}^{2+}$  are shorter in comparison to the distances in their analogues of **1a**. As an example, the N- $\text{Be}^{2+}$  distances in **1b**<sub>Be<sup>2+</sup></sub> are shorter by 0.017 Å than in **1a**<sub>Be<sup>2+</sup></sub>. The C(Py)-NMe<sub>2</sub> bond distances are shortened upon complexation because of the lone-pair back donation in conjunction with the cationic resonance, which occurs at the expense of a decreased hyperconjugation effect between the amino nitrogen and the methyl groups, which are, in turn, increased by a small but significant amount (Figure S22 - S28).





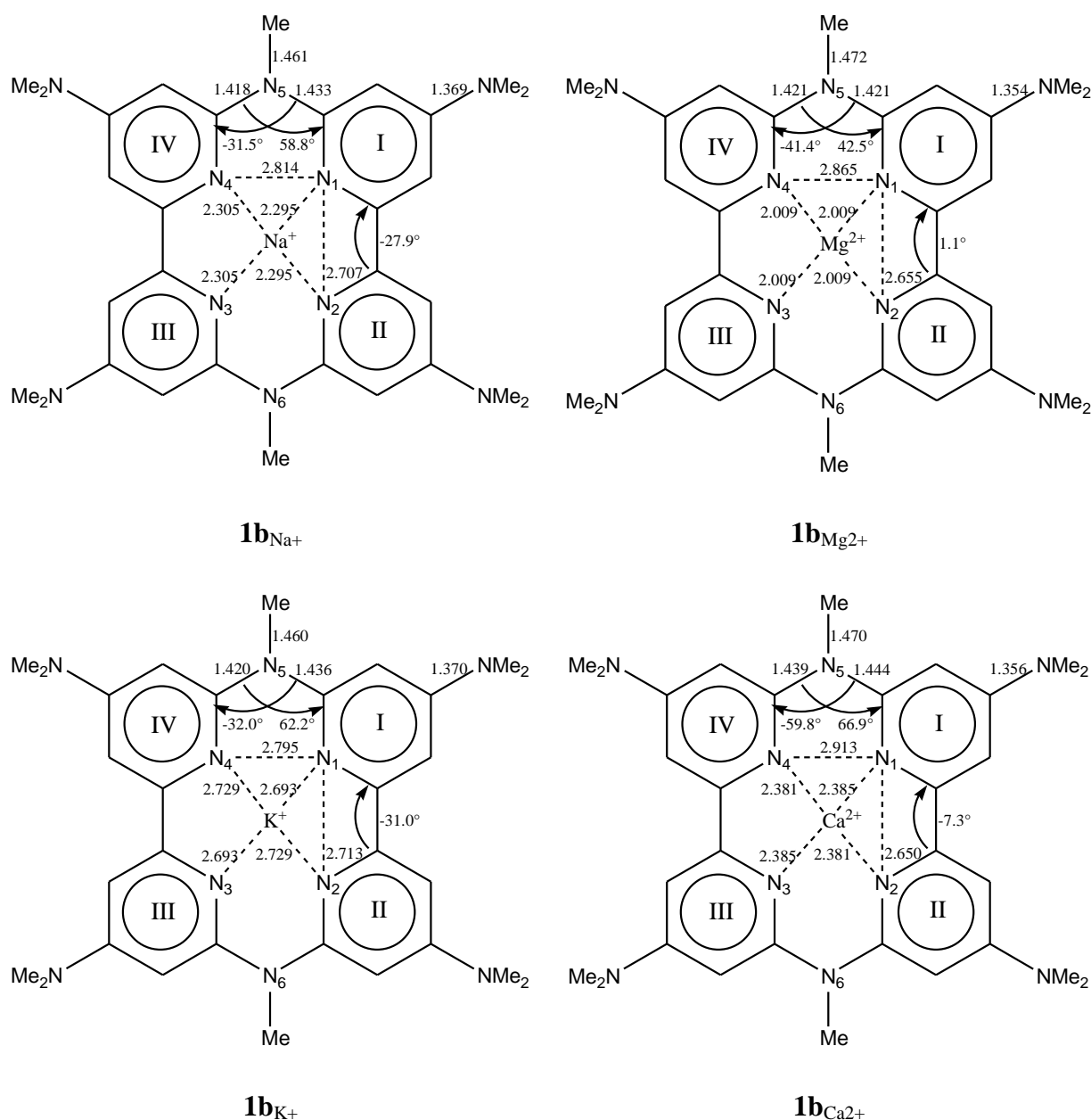
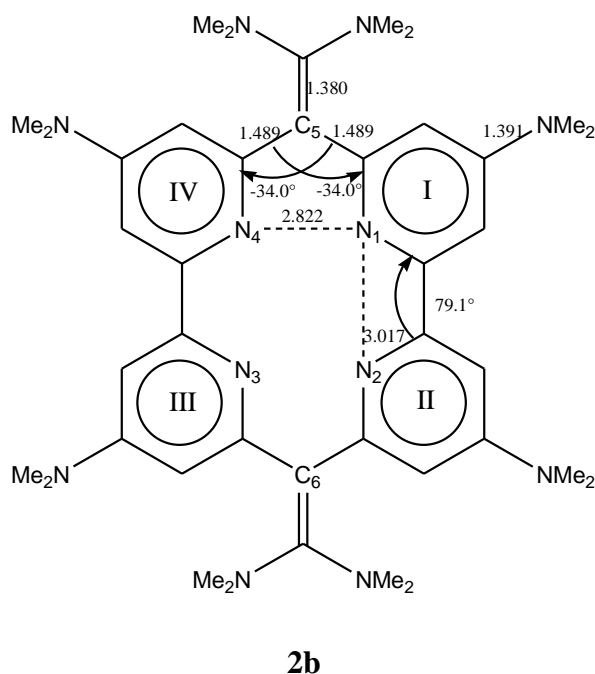


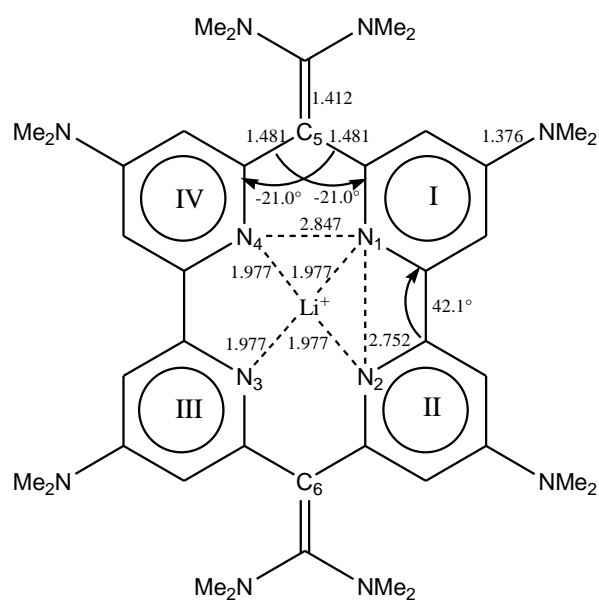
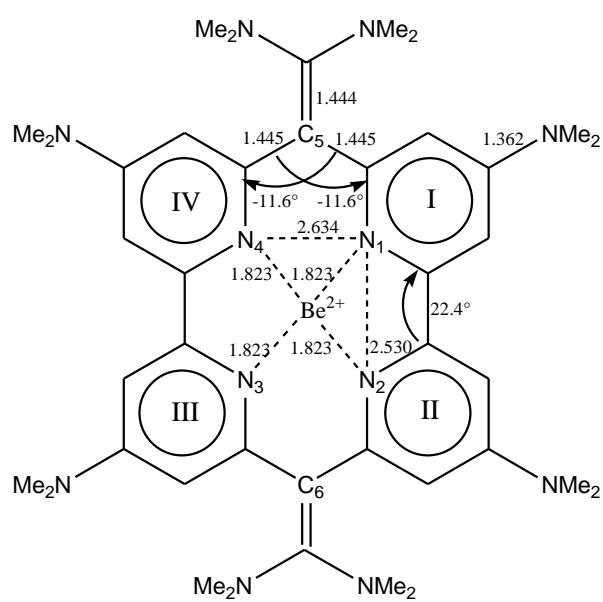
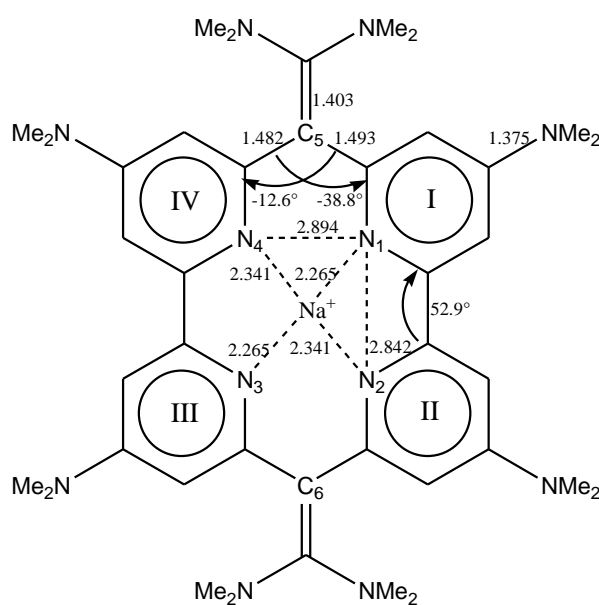
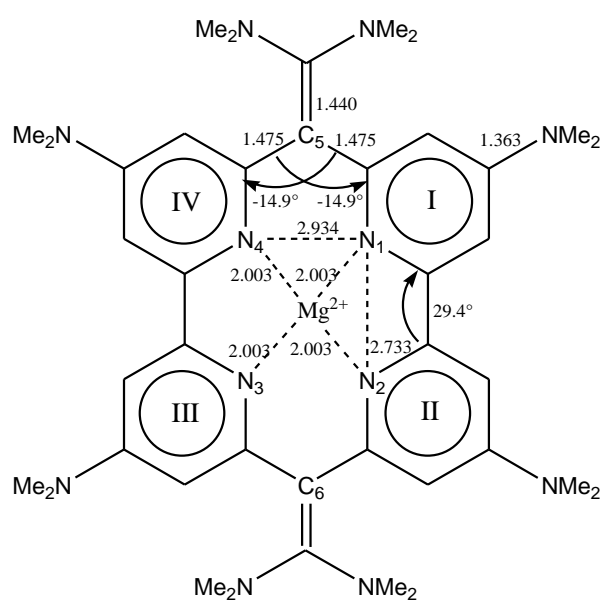
**Figure 4** Some relevant structural parameters of supramolecule **1b** and its complexes with  $\text{Li}^+$ ,  $\text{Na}^+$ ,  $\text{K}^+$ ,  $\text{Be}^{2+}$ ,  $\text{Mg}^{2+}$  and  $\text{Ca}^{2+}$  (bond distances are given in Å).

The structural patterns in **2b** and its complexes (Figure 5, Figure S36-S42) are similar to those of **1b**, **1b**<sub>Li<sup>+</sup></sub>, **1b**<sub>Na<sup>+</sup></sub>, **1b**<sub>K<sup>+</sup></sub>, **2b**<sub>Be<sup>2+</sup></sub>, **2b**<sub>Mg<sup>2+</sup></sub> and **2b**<sub>Ca<sup>2+</sup></sub>, respectively, but there are some notable differences. In the first place, **2b** is less strained, having larger N $\cdots$ N distances. The double bond C5=C(NMe<sub>2</sub>)<sub>2</sub> at the bridged C atom is considerably twisted, as evidenced by the dihedral angle C(I)-C5=C-N(Me<sub>2</sub>) of -30.5°. The dihedral angle between the directly connected pyridine rings and the nonbonded N $\cdots$ N distance are larger in **2b** than in **1b**,

which is also true for their complexes. The distances between the metal cation and the pyridine nitrogens are larger in **2b**<sub>Li+</sub>, **2b**<sub>Na+</sub>, **2b**<sub>K+</sub> and **2b**<sub>Be2+</sub> than in their **1b** counterparts, while in **2b**<sub>Mg2+</sub> and **2b**<sub>Ca2+</sub> these distances are shorter than in **1b**<sub>Mg2+</sub> and **1b**<sub>Ca2+</sub>. The C(Py) – N(Me<sub>2</sub>) distances are shortened upon complexation, as in the **1b** complexes. The resonance effect also occurs within the *bis*(dimethylamino) substituted double bond at the expense of a decreased hyperconjugation effect between the amino nitrogen and carbon atoms in the NMe<sub>2</sub> fragments, which is evidenced by an increase of the bond distances between the nitrogen and carbon atoms, by a small but significantly amount.

In order to shed further light on this matter, let us consider the electron density distribution in the complexes in which +1 or +2 charge is shared by the cation and macrocyclic ligand. It is well known that the cation located in the center of the macrocyclic ring, surrounded by electron donors, is held there principally by electrostatic, i.e. ion-dipole forces. Furthermore, the charge-dipole interactions, as all other stabilization forces, diminish with increasing ion-dipole distance. They are, therefore, significantly more important for smaller ions which are able, due to their size, to be closer to the electron-donor atoms.



**2b**<sub>Li<sup>+</sup></sub>**2b**<sub>Be<sup>2+</sup></sub>**2b**<sub>Na<sup>+</sup></sub>**2b**<sub>Mg<sup>2+</sup></sub>

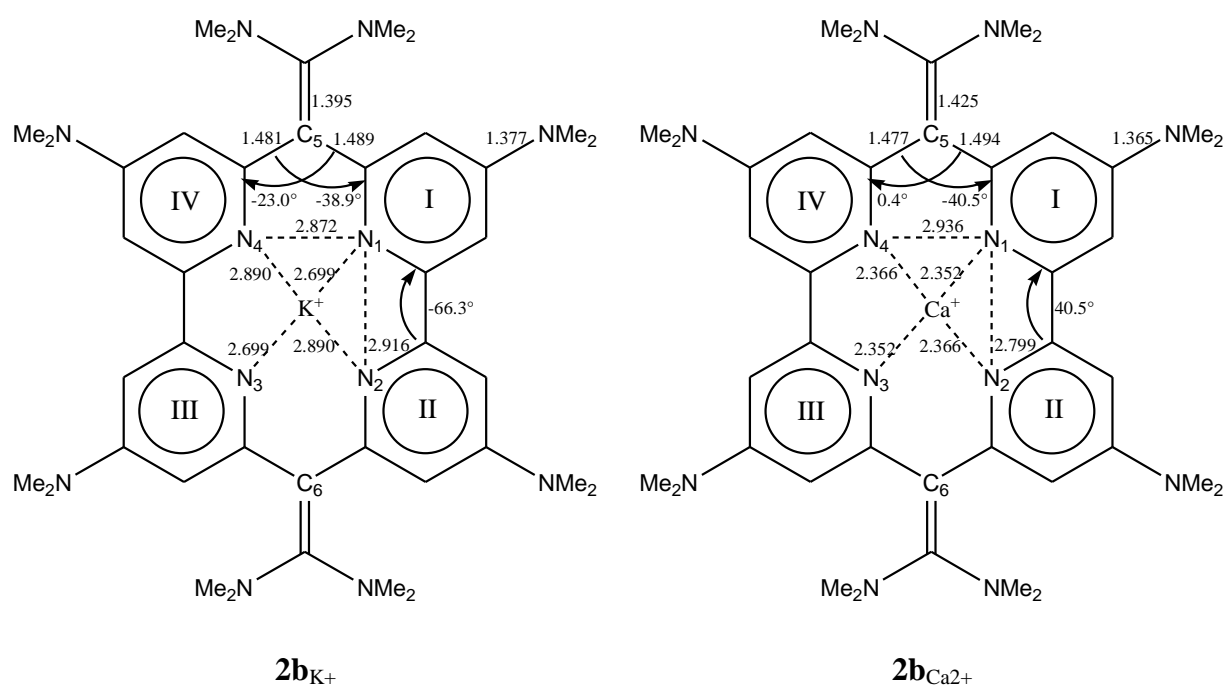


**Figure 5** Some relevant structural parameters of supramolecule **2b** and its complexes with  $Li^+$ ,  $Na^+$ ,  $K^+$ ,  $Be^{2+}$ ,  $Mg^{2+}$  and  $Ca^{2+}$  (bond distances are given in Å).

All cations are Lewis acids, and therefore, electron acceptors. When attached to an electron donating site, this will lead to some Lewis acid - base interaction or, in other words, partial electron transfer from electron donor to the metal cation. In this context, the relevant property of the metal ion is its electron affinity (EA). In a complex with a metal cation of high EA, a larger charge transfer takes place.<sup>28</sup> There are several ways to define the effective charges of atoms in molecules. The results are not unique, and the question is which criterion has to be chosen. We employed here Hirshfeld's atomic densities obtained by the stockholder principle.<sup>38</sup> It provides one of the most reliable ways of describing electron redistribution in the molecules.<sup>39</sup> The qualitative insight in the strength of the bonds is offered by employing the bond order of Mayer.<sup>40</sup> The atomic densities of the cations in question, and the pyridine nitrogens, are given in Table 2, together with the bond orders of  $N-M^{+/2+}$ .

One observes that  $Be^{2+}$  attracts the largest portion of the electron density in the amount of 1.66  $e$ , 1.70  $e$ , 1.68  $e$  and 1.70  $e$  in **1a** <sub>$Be^{2+}$</sub> , **1b** <sub>$Be^{2+}$</sub> , **2a** <sub>$Be^{2+}$</sub>  and **2b** <sub>$Be^{2+}$</sub> , respectively. These results are fully in line with the very high electron affinity (523.0 kcal mol<sup>-1</sup>) of  $Be^{2+}$ . The  $Mg^{2+}$  cation attracts a slightly lower amount of electron density (1.42  $e$ , 1.44  $e$ , 1.48  $e$  and 1.50  $e$  in **1a** <sub>$Mg^{2+}$</sub> , **1b** <sub>$Mg^{2+}$</sub> , **2a** <sub>$Mg^{2+}$</sub>  and **2b** <sub>$Mg^{2+}$</sub> , respectively), which is to be intuitively expected,

due to the lower electron affinity of the  $\text{Mg}^{2+}$  cation compared to the electron affinity of the  $\text{Be}^{2+}$  cation. The amount of 1.24  $e$ , 1.28  $e$ , 1.32  $e$  and 1.35  $e$  is transferred from pyridine nitrogens to the  $\text{Ca}^{2+}$  cations in **1a**<sub>Ca2+</sub>, **1b**<sub>Ca2+</sub>, **2a**<sub>Ca2+</sub> and **2b**<sub>Ca2+</sub>, respectively, being lower than that in the  $\text{Mg}^{2+}$  complexes. For alkali cations the electron affinities are smaller and decrease in the same way, in order from  $\text{Li}^+$  to  $\text{K}^+$ . This is evidenced in lower density transfer in the  $\text{Li}^+$ ,  $\text{Na}^+$  and  $\text{K}^+$  complexes (Table 2), which was intuitively expected. It has to be noted that these values are roughly two or three times larger compared to those of the corresponding complexes of the building block pyridine molecule (Figure 2) with the metal cation. The population analysis reveals that the variations of the effective pyridine nitrogen charges upon complexation are almost negligible. This counterintuitive observation indicates that the formation of the  $\text{N-M}^{+/2+}$  bond induces a full rearrangement of the electron density inside the aromatic ring, so that upon complexation, all C atoms of the pyridine ring donate their electrons to the nitrogen atom (Table S3).

Inspection of Mayer's bond orders (Table 2) reveals that medium strength covalent interactions with the four pyridine N atoms are found in complexes with the  $\text{Be}^{2+}$  cation. Their combination with Coulomb attraction yields high cationic affinities. The interaction with  $\text{Li}^+$ ,  $\text{Mg}^{2+}$  and  $\text{Ca}^{2+}$  cations are of a more electrostatic nature, while the smallest covalent interactions were found in  $\text{Na}^+$  and  $\text{K}^+$  complexes, as intuitively expected.

**Table 2** Atomic populations obtained by the Hirshfeld population analysis (in  $e$ ) for the complexed cations and pyridine nitrogens, and Mayer bond order of the  $\text{N-M}^{+/2+}$

Compd	$\text{M}^{+/2+}$	N1	N2	N3	N4	N1- $\text{M}^{+/2+}$	N2- $\text{M}^{+/2+}$	N3- $\text{M}^{+/2+}$	N4- $\text{M}^{+/2+}$
<b>1a</b>	-	7.18	7.18	7.18	7.18	-	-	-	-
<b>1a</b> <sub>Li+</sub>	2.80	7.18	7.18	7.18	7.18	0.20	0.19	0.20	0.19
<b>1a</b> <sub>Na+</sub>	10.64	7.16	7.18	7.16	7.18	0.06	0.06	0.06	0.06
<b>1a</b> <sub>K+</sub>	18.53	7.19	7.21	7.19	7.21	0.05	0.06	0.05	0.06
<b>1a</b> <sub>Be2+</sub>	3.66	7.14	7.14	7.14	7.14	0.44	0.44	0.44	0.44
<b>1a</b> <sub>Mg2+</sub>	11.42	7.18	7.18	7.18	7.18	0.27	0.27	0.27	0.27
<b>1a</b> <sub>Ca2+</sub>	19.24	7.18	7.18	7.18	7.18	0.15	0.15	0.15	0.15

<b>1b</b>	-	7.20	7.20	7.20	7.20	-	-	-	-
<b>1b<sub>Li+</sub></b>	2.80	7.20	7.20	7.20	7.20	0.22	0.21	0.22	0.21
<b>1b<sub>Na+</sub></b>	10.66	7.20	7.20	7.20	7.20	0.07	0.07	0.07	0.07
<b>1b<sub>K+</sub></b>	18.55	7.24	7.22	7.24	7.22	0.05	0.07	0.05	0.07
<b>1b<sub>Be2+</sub></b>	3.70	7.16	7.16	7.16	7.16	0.46	0.46	0.46	0.46
<b>1b<sub>Mg2+</sub></b>	11.44	7.20	7.20	7.20	7.20	0.27	0.27	0.27	0.27
<b>1b<sub>Ca2+</sub></b>	19.28	7.21	7.21	7.21	7.21	0.16	0.16	0.16	0.16
<b>2a</b>	-	7.18	7.18	7.18	7.18	-	-	-	-
<b>2a<sub>Li+</sub></b>	2.82	7.18	7.18	7.18	7.18	0.24	0.24	0.24	0.24
<b>2a<sub>Na+</sub></b>	10.70	7.18	7.18	7.18	7.18	0.08	0.09	0.08	0.09
<b>2a<sub>K+</sub></b>	18.57	7.21	7.21	7.21	7.21	0.05	0.08	0.05	0.08
<b>2a<sub>Be2+</sub></b>	3.68	7.14	7.14	7.14	7.14	0.45	0.45	0.45	0.45
<b>2a<sub>Mg2+</sub></b>	11.48	7.20	7.20	7.20	7.20	0.35	0.35	0.35	0.35
<b>2a<sub>Ca2+</sub></b>	19.32	7.19	7.20	7.19	7.20	0.18	0.19	0.18	0.19
<b>2b</b>	-	7.20	7.20	7.20	7.20	-	-	-	-
<b>2b<sub>Li+</sub></b>	2.82	7.20	7.20	7.20	7.20	0.25	0.25	0.25	0.25
<b>2b<sub>Na+</sub></b>	10.70	7.20	7.20	7.20	7.20	0.10	0.10	0.10	0.10
<b>2b<sub>K+</sub></b>	18.61	7.24	7.24	7.24	7.24	0.05	0.09	0.05	0.09
<b>2b<sub>Be2+</sub></b>	3.70	7.16	7.16	7.16	7.16	0.46	0.46	0.46	0.46
<b>2b<sub>Mg2+</sub></b>	11.50	7.22	7.22	7.22	7.22	0.37	0.37	0.37	0.37
<b>2b<sub>Ca2+</sub></b>	19.35	7.22	7.22	7.22	7.22	0.19	0.20	0.19	0.20

### 3.2. Complexation in acetonitrile

The stability constants ( $\log K$ ) are given in Table 3. The continuum solvation free energies of the neutral ligands **1a** – **2b** and their positively charged complexes with one AN molecule included into the coordination sphere around the metal cation, as well as that of the clustered metal ion with four AN molecules, are given in Table S4. The Gibbs reaction free energies in acetonitrile solution,  $\Delta_r G^*_{(\text{AN})}$ , are given in Table S5.

**Table 3** The stability constants ( $\log K$ ) of complexes of **1a** - **2b** with  $\text{Li}^+$ ,  $\text{Na}^+$ ,  $\text{K}^+$ ,  $\text{Be}^{2+}$ ,  $\text{Mg}^{2+}$  and  $\text{Ca}^{2+}$  cations.

Host compound	$\log K$					
	$\text{Li}^+$	$\text{Na}^+$	$\text{K}^+$	$\text{Be}^{2+}$	$\text{Mg}^{2+}$	$\text{Ca}^{2+}$
<b>1a</b>	21.12	13.40	8.60	38.11	36.05	23.37
<b>1b</b>	24.68	16.80	10.93	49.64	45.99	30.61
<b>2a</b>	20.51	14.26	8.36	41.73	41.77	23.48
<b>2b</b>	24.68	17.32	10.45	52.05	51.74	32.19

Perusal of the data in Table 3 reveals that the trend in gas-phase complexation is well-preserved in acetonitrile. One notices that, in **2a**<sub>Be2+</sub> and **2a**<sub>Mg2+</sub>, the complex stabilities are almost of the same magnitude, which is also true for **2a**<sub>Be2+</sub> and **2a**<sub>Mg2+</sub>. The stability constants are calculated to span the range between 8.36 and 24.68 units for monocations  $\text{Li}^+$  to  $\text{K}^+$ , and between 23.37 and 52.05 units for dications  $\text{Be}^{2+}$  to  $\text{Ca}^{2+}$ . These values indicate strong complexing activity of the ligands **1a** - **2b** in acetonitrile, culminating with the exceptional stability constant for **2b**<sub>Be2+</sub> of 52.05 units.

On the basis of given data it is fair to say that macrocyclic systems **1a** - **2b** are (a) efficient and (b) selective ligands for the considered metal cations in acetonitrile solution.

Given the growing interest in design and use of the metal complexing agents, we hope that the results presented here would open new direction of research in these fields.

#### 4. Concluding Remarks

The  $\text{Li}^+$ ,  $\text{Na}^+$ ,  $\text{K}^+$ ,  $\text{Be}^{2+}$ ,  $\text{Mg}^{2+}$  and  $\text{Ca}^{2+}$  affinities and basicities of **1a** - **2b** pyridine-based macrocyclic ligands were calculated using the DFT B3LYP/6-311+G(3df,2p)//B3LYP/6-31G(d) method. It has been shown that investigated macrocyclic compounds **1a** - **2b** are good complexing and very selective ligands, exhibiting gas phase cation affinities lying in the range between 58.5 kcal mol<sup>-1</sup> and 553.8 kcal mol<sup>-1</sup>. The most stable complexes are provided by the tetrasubstituted macrocyclic system **2b**.

The highly rigid and well preorganized macrocyclic ligands act in a cooperative tetradentate fashion, providing four pyridine nitrogen atoms to bind to a central atom in the coordination complex. The highest values of the cation affinities are found to be towards the  $\text{Be}^{2+}$  cation, which possesses the smallest radius, enabling its perfect fitting within the macrocyclic ion-binding site, and a very high electron affinity. On the contrary, the lowest values of the cation affinities are found for the  $\text{K}^+$  cation, possessing the highest atomic radius, which causes a protrusion from the binding site, and a considerably lower electron affinity compared to the  $\text{Be}^{2+}$  cation. Based on these results, it is clear that the cation affinities of the ligands **1a** - **2b** are well correlated with the radius and the electron affinity of the complexed metal cation. The CA increases with the decrease of the radius and with the increase of the electron affinity of the metal cation, in the order  $\text{K}^+ < \text{Na}^+ < \text{Li}^+ < \text{Ca}^{2+} < \text{Mg}^{2+} < \text{Be}^{2+}$ . The structural analysis of the complexes revealed planarization of the macrocyclic ring upon complexation, being the most pronounced in  $\text{Be}^{2+}$  complexes.

The cation affinity of the hosts has been amplified by attaching the electron-donating  $\text{NMe}_2$  group on the pyridine rings. The reason for this is considered to be due to the electron releasing property of the nitrogen lone pair of the  $\text{NMe}_2$  group and its contribution to the cationic resonance, triggered by metal cation complexation. The changes in cation affinity as a consequence of the  $\text{NMe}_2$  substitution are most pronounced in complexes with the  $\text{Be}^{2+}$  metal cation.

The amount of charge transferred from the pyridine nitrogens to the metal cation is correlated with metal cation affinity, which means that the highest charge transfer is found in  $\text{Be}^{2+}$  complexes while the lowest charge transfer takes place in  $\text{K}^+$  complexes. It is interesting to note that pyridine nitrogens retrieve all electron density lost to trapped cations. Medium strength covalent interaction with four pyridine nitrogen atoms is found in complexes with



Be<sup>2+</sup> cation. The smallest covalent interaction was found in K<sup>+</sup> complexes, as intuitively expected.

The metal cation binding in acetonitrile solution was examined. In general, the trend in the gas phase binding is well preserved in acetonitrile solution. The stability constants are calculated to span the range between 8.36 and 52.05 units. The highest stability constant is found in the **2**<sub>Be2+</sub> system.

One can safely state that pyridine-based supramolecular structures **1** and **2** offer useful ligands capable of efficient and selective sequestration of cations Li<sup>+</sup>, Na<sup>+</sup>, K<sup>+</sup>, Be<sup>2+</sup>, Mg<sup>2+</sup> and Ca<sup>2+</sup>. Thus their syntheses are strongly recommended.

## Acknowledgements

This work was financially supported by the Ministry of Science, Education and Sports of the Republic of Croatia through Grant No. 098-0982933-2932. I would like to thank the University of Zagreb Computing Centre (SRCE) for a generously granting computational resources on the ISABELLA cluster (isabella.srce.hr).

## Supplementary data

Supplementary data related to this article can be found at

## References and notes

---

<sup>1</sup> C. J. Pedersen, *J. Am. Chem. Soc.* 1967, **89**, 7017.

<sup>2</sup> (a) R. M. Izatt, J. S. Bradshaw, S. A. Nielson, J. D. Lamb, J. J. Christensen, D. Sen, *Chem. Rev.* 1985, **85**, 271; (b) E. D. Glendening, D. Feller, M. A. Thompson, *J. Am. Chem. Soc.* 1994, **116**, 10657, (c) J. M. Lehn, *Supramolecular chemistry*; VCH: Weinheim, 1995; (d) E. D. Glendening, D. Feller, *J. Am. Chem. Soc.* 1996, **118**, 6052, (e) R. Puchta, V. Seitz, N. J. R. van Eikema Hommes, R. W. Saalfrank, *J. Mol. Model.* 2000, **6**, 126, (f) Smith, M. B.; March, J. *March's Advanced Organic Chemistry*, 5<sup>th</sup> ed., Wiley: New York, 2001, (g) R. Puchta, R. van Eldik, *Eur. J. Inorg. Chem.* 2007, 1120, (h) E. Pasgreta, R. Puchta, A. Zahl, R. van Eldik, *Eur. J. Inorg. Chem.* 2007, 3067, (i) R. Puchta, R. Meier, R. van Eldik, *Aust. J. Chem.* 2007, **60**, 889, (j) R. Puchta, R. van Eldik, *J. Incl. Phenom. Macrocycl. Chem.* 2008, **60**, 383, (k) R.

Puchta, B. Roling, A. Scheurer, V. Weiskopf, F. Hampel, N. J. R. van Eikema Hommes, H.-U. Hummel, *Solid State Ionics* 2008, **179**, 489, (l) S. Begel, R. Puchta, R. van Eldik, *Beilstein J. Org. Chem.* 2013, **9**, 1252, (m) S. Begel, R. Puchta, R. van Eldik, *J. Mol. Model.* 2014, **20**, 220.

<sup>3</sup> (a) H. M. Betts, S. I. Pascu, A. Buchard, P. D. Bonnitcho, J. R. Dilworth, *RSC Adv.* 2014, **4**, 12964; (b) A. Melchior, E. Peralta, M. Valiente, C. Tavagnacco, F. Endrizzi, M. Tolazzi, *Dalton Trans.* 2013, **42**, 6074; (c) P. Kandwal, S. A. Ansari, P. K. Mohaparta, *J. Membr. Sci.* 2011, **384**, 37.

<sup>4</sup> (a) P. Bühlmann, E. Pretsch, E. Bakker, *Chem. Rev.* 1998, **98**, 1593; (b) A. Melchior, E. Peralta, M. Valiente, M. Tolazzi, *Polyhedron* 2014, **75**, 88; (c) R. D. Hancock, L. J. Bartolotti, *Inorg. Chim. Acta* 2013, **396**, 101; (d) V. Bhalla, R. Tejpal, M. Kumar, *Dalton Trans.* 2012, **41**, 10182; (e) G. J. Grant, N. N. Talbott, M. Bajic, L. F. Mehne, T. J. Holcombe, D. G. VanDerveer, *Polyhedron* 2012, **31**, 89; (f) G. J. Grant, *Dalton Trans.* 2012, **41**, 8745; (g) J. F. Zhang, Y. Zhou, J. Yoon, J. S. Kim, *Chem. Soc. Rev.* 2011, **40**, 3416; (h) X. Li, R. Z. Liao, W. Zhou, G. Chen, *Phys. Chem. Chem. Phys.* 2010, **12**, 3961; (i) T. Chen, W. P. Zhu, Y. F. Xu, S. Y. Zhang, X. J. Zhang, X. H. Qian, *Dalton Trans.* 2010, **39**, 1316; Müller, H.; Kelling, H.; Schilde, U.; Holdt, H. J. *Z. Naturforsch* 2009, **64b**, 1003; (j) G. J. Grant, D. A. Benefield, D. G. VanDerveer, *Dalton Trans.* 2009, 8605; (k) M. Aragoni, M. Arca, A. Bencini, S. Biagini, A. J. Blake, C. Catagirone, F. Demartin, G. De Filippo, F. A. Devillanova, A. Garau, K. Globe, F. Isaia, V. Lipollis, B. Vatancoli, M. Wenzel, *Inorg. Chem.* 2008, **47**, 8391.

<sup>5</sup> (a) H. Bakirci, A. L. Koner, M. H. Dickman, U. Kortz, W. M. Nau, *Angew. Chem. Int. Ed.* 2006, **45**, 7400; (b) R. E. Mewis, S. J. Archibald, *Coord. Chem. Rev.* 2010, **254**, 1686.

<sup>6</sup> (a) C.-C. Lee, H.-C. Huang, S.-T. Liu, Y.-H. Liu, S.-M. Peng, J.-T. Chen, *Polyhedron* 2013, **52**, 1024; (b) H. Zhu, S. J. Paddison, T. A. Zawodzinski Jr., *Electrochimica Acta* 2013, **101**, 293; (c) H. J. Yoon, J. Kuwabara, J.-H. Kim, C. A. Mirkin, *Science*, 2010, **330**, 66-69; (d) R. Gerdes, L. Lapok, O. Tsaryova, D. Wöhrle, M. S. Gorun, *Dalton Trans.* 2009, 1098.

<sup>7</sup> P. J. Panak, A. Geist, *Chem. Rev.* 2013, **113**, 1199.

<sup>8</sup> P. Faller, C. Hureau, *Dalton Trans.* 2009, 1080.

<sup>9</sup> (a) K. M. Lincoln, M. E. Offut, T. D. Hayden, R. E. Saunders, K. N. Green, *Inorg. Chem.* 2014, **53**, 1406; (b) C.-Y. Gao, L. Zhao, M.-X. Wang, *J. Am. Chem. Soc.* 2012, **134**, 824; (c) V. Guerschais, J.-L. Fillaut, *Coord. Chem. Rev.* 2011, **255**, 2448; (d) A. S. Fernandes, M. F. Cabral, J. Costa, M. Castro, R. Delgado, M. G. B. Drew, V. Felix, *J. Inorg. Biochem.* 2011, **105**, 410; (e) C. Núñez, R. Bastida, A. Macías, A. Aldrey, L. Valencia, *Polyhedron* 2010, **29**, 126.

<sup>10</sup> M. Razaivala, H. Keypour, *Coord. Chem. Rev.* 2014, **280**, 203.

<sup>11</sup> (a) Y. Miyazaki, T. Kanbara, T. Yamamoto, *Tetrahedron Lett.* 2002, **43**, 7945; (b) Y. Suzuki, T. Yanagi, T. Kanbara, T. Yamamoto, *Synlett* 2005, 0263.

<sup>12</sup> I. Despotović, Z. B. Maksić, *Tetrahedron Lett.* 2011, **52**, 6263.

<sup>13</sup> B. Kovačević, I. Despotović, Z. B. Maksić, *Tetrahedron Lett.* 2007, **48**, 261.

<sup>14</sup> (a) A. D. Becke, *Phys. Rev. A* 1988, **38**, 3098; (b) C. Lee, M. Yang, R. G. Parr, *Phys. Rev. B* 1988, **37**, 785; (c) P. J. Stephens, F. J. Devlin, C. F. Chabalowski, M. J. Frisch, *J. Phys. Chem.* 1994, **98**, 11623.

<sup>15</sup> (a) C. W. Bauschlicher Jr., H. Partridge, *J. Chem. Phys.* 1995, **103**, 1788, (b) L. A. Curtiss, P. C. Redfern, K. Raghavachari, J. A. Pople, *J. Chem. Phys.* 2001, **114**, 108, (c) O. Mó, M. Yáñez, J.-Y. Salpin, J. Tortajada, *Mass. Spectrom. Rev.* 2007, **26**, 474.

<sup>16</sup> J. F. Gal, P.-C. Maria, O. Mó, M. Yáñez, D. Kuck, *Chem. Eur. J.* 2006, **12**, 7676.

- <sup>17</sup> S. F. Boys, F. Bernardi, *Mol. Phys.* 1970, **19**, 553.
- <sup>18</sup> (a) S. Miertuš, E. Scrocco, J. Tomasi, *J. Chem. Phys.* 1981, **55**, 117; (b) S. Miertuš, J. Tomasi, *J. Chem. Phys.* 1982, **65**, 239.
- <sup>19</sup> R. F. Ribeiro, A. V. Marenich, C. J. Cramer, D. G. Truhlar, *J. Phys. Chem. B* 2011, **115**, 14556.
- <sup>20</sup> Y. Inada, Y. Nakayama, S. Funahashi, *J. Solution Chem.* 2004, **33**, 847.
- <sup>21</sup> Due to the consistency in the theoretical approach the first coordination shell of the all metal cations investigated were modelled by four AN molecules.
- <sup>22</sup> J. R. Pliego, Jr., J. M. Riveros, *J. Phys. Chem. A* 2001, **105**, 7241.
- <sup>23</sup> (a) P. Groth, *Acta Chem. Scand. A* 1981, **35**, 463; (b) B. R. Gibney, H. Wang, J. W. Kampf, V. L. Pecoraro, *Inorg. Chem.* 1996, **35**, 6184; (c) B. Neumüller, K. Dehnicke, *Z. Anorg. Allg. Chem.* 2006, **632**, 1681;
- <sup>24</sup> C. P. Kelly, C. J. Cramer, D. G. Truhlar, *J. Chem. Theory Comput.* 2005, **1**, 1133.
- <sup>25</sup> M. J. Frisch, G. W. Trucks, H. B. Schlegel, G. E. Scuseria, M. A. Robb, J. R. Cheeseman, J. A. Montgomery, Jr, T. Vreven, K. N. Kudin, J. C. Burant, J. M. Millam, S. S. Iyengar, J. Tomasi, V. Barone, B. Mennucci, M. Cossi, G. Scalmani, N. Rega, G. A. Petersson, H. Nakatsuji, M. Hada, M. Ehara, K. Toyota, R. Fukuda, J. Hasegawa, M. Ishida, T. Nakajima, Y. Honda, O. Kitao, H. Nakai, M. Klene, X. Li, J. E. Knox, H. P. Hratchian, J. B. Cross, V. Bakken, C. Adamo, J. Jaramillo, R. Gomperts, R. E. Stratmann, O. Yazyev, A. J. Austin, R. Cammi, C. Pomelli, J. W. Ochterski, P. Y. Ayala, K. Morokuma, G. A. Voth, P. Salvador, J. J. Dannenberg, V. G. Zakrzewski, S. Dapprich, A. D. Daniels, M. C. Strain, O. Farkas, D. K. Malick, A. D. Rabuck, K. Raghavachari, J. B. Foresman, J. V. Ortiz, Q. Cui, A. G. Baboul, S. Clifford, J. Cioslowski, B. B. Stefanov, G. Liu, A. Liashenko, P. Piskorz, I. Komaromi, R. L. Martin, D. J. Fox, T. Keith, M. A. Al-Laham, C. Y. Peng, A. Nanayakkara, M. Challacombe, P. M. W. Gill, B. Johnson, W. Chen, M. W. Wong, C. Gonzalez, J. A. Pople, *Gaussian 03*, revision B.03, Gaussian, Inc., Wallingford CT, 2004.
- <sup>26</sup> G. Schwarzenbach, *Helv. Chim. Acta* 1952, **35**, 2344.
- <sup>27</sup> D. K. Cabbiness, D. W. Margerum, *J. Am. Chem. Soc.* 1969, **91**, 6540.
- <sup>28</sup> D. J. Cram, J. M. Cram, *Acc. Chem. Res.*, 1978, **11**, 8.
- <sup>29</sup> L. F. Lindoy, *The Chemistry of Macrocyclic Ligand Complexes*; Cambridge University Press; Cambridge, 1989, pp 4-6, 185-191.
- <sup>30</sup> (a) R. D. Hancock, S. M. Dobson, A. Evers, P. W. Wade, M. P. Ngwenya, J. C. A. Boeyens, K. P. Wainwright, *J. Am. Chem. Soc.* 1988, **110**, 2788, (b) R. D. Hancock, *Acc. Chem. Res.* 1990, **23**, 253.
- <sup>31</sup> R. D. Hancock, A. E. Martell, *Chem. Rev.* 1989, **89**, 1875.
- <sup>32</sup> J. E. Sansonetti, W. C. Martin, S. L. Young, *J. Phys. Chem. Rev. Data* 2005, **34**, 1559..
- <sup>33</sup> R. D. Shannon, *Acta Cryst.* 1976, **A32**, 751.
- <sup>34</sup> (a) Z. Yang, M. T. Rodgers, *J. Phys. Chem. A* 2006, **110**, 1455; (b) H. Roohi, E. Zahiri, *Comput. Theor. Chem.* 2012, **984**, 113; (c) B. Khalili, M. Rimaz, T. Tondro, *J. Mol. Struct.* 2015, **1080**, 80.
- <sup>35</sup> T. Marino, N. Russo, M. Toscano, *J. Phys. Chem. B* 2003, **107**, 2588.
- <sup>36</sup> (a) E. D. Glendening, D. Feller, M. A. Thompson, *J. Am. Chem. Soc.* 1994, **121**, 10657; (b) M. B. More, D. Ray, P. B. Armentrout, *J. Am. Chem. Soc.* 1999, **121**, 417; (c) P. B. Armentrout, *Int. J. Mass. Spectrom.* 1999, **193**, 227.
- <sup>37</sup> (a) F. H. Allen, *Acta Crystallogr., Sect. B: Struct. Sci.* 2002, **58**, 380; (b) Cambridge Structure Database, Version 53, 2011.
- <sup>38</sup> F. L. Hirshfeld, *Theor. Chim. Acta* 1977, **44**, 129.

---

<sup>39</sup> For a detailed analysis see: K. Jug, Z. B. Maksić, In Theoretical Models of Chemical Bonding, Part 3, Z. B. Maksić, Ed., Springer Verlag, Heidelberg- berlin, 1991, pp. 235-288.

<sup>40</sup> I. Mayer, *Chem. Phys. Lett.* 1983, **97**, 270; (b) I. Mayer, *J. Comput. Chem.* 2007, **28**, 204.